Appl Phys B (2009) 97: 505–510
DOI 10.1007/s00340-009-3559-z

Applied Physics B
Lasers and Optics

Four-dimensional investigation of the 2nd order volume autocorrelation technique

O. Faucher · P. Tzallas · E.P. Benis · J. Kruse · A. Peralta Conde · C. Kalpouzos · D. Charalambidis

Received: 10 February 2009 / Published online: 2 May 2009

Abstract The 2nd order volume autocorrelation technique, widely utilized in directly measuring ultra-short light pulses durations, is examined in detail via model calculations that include three-dimensional integration over a large ionization volume, temporal delay and spatial displacement of the two beams of the autocorrelator at the focus. The effects of the inherent displacement to the 2nd order autocorrelation technique are demonstrated for short and long pulses, elucidating the appropriate implementation of the technique in tight focusing conditions. Based on the above investigations, a high accuracy 2nd order volume autocorrelation measurement of the duration of the 5th harmonic of a 50 fs long laser pulse, including the measurement of the carrier wavelength oscillation, is presented.

PACS 42.65.Ky · 42.65.Re · 32.80.Rm

1 Introduction

The measurement of the duration of an ultra-short radiation pulse or determination of the characteristic time of an ultra-fast process relies on a non-linear process. During the last decade, the well established in femtosecond (fs) metrology 2nd order autocorrelation (AC) technique has been successfully extended to the ultra-violet (UV) and extreme ultra-violet (EUV) spectral regions, serving for the temporal characterization of pulses in the attosecond (as) time scale [1–3]. 2nd order AC is a method that directly and safely determines the temporal duration of as pulses. Once established, it becomes straightforward provided that sufficient EUV intensity is available.

Apart from the generation of as EUV radiation and its applications to attophysics and attochemistry [4, 5], the availability of intense few-fs UV-EUV pulses is of potential importance to the study of the dynamics of photochemical reactions [6, 7], in view of the fact that most of the organic compounds absorb in this spectral region. Towards this target, sub-10 fs UV and EUV pulses can be for instance generated through the interaction of a gas phase medium with high-peak-power few-cycle laser pulses [8, 9] or with many-cycle laser pulses of appropriately tailored polarization utilizing the interferometric polarization gating technique [10, 11]. In certain cases though, even UV-EUV pulses of a few tens of fs would be sufficiently short to study various photochemical processes [12]. A prerequisite for a thorough quantitative study of the above dynamics is the most accurate knowledge of the duration of the EUV pulse, which is straightforwardly accessible by the 2nd order AC technique.

In this work, we present numerical results for the applicability conditions of the 2nd order AC approach obtained by model calculations that include not only three-dimensional integration over a large ionization volume and temporal delay, but also spatial displacement of the two beams of the autocorrelator at the focus. In contrast to all previous works,

O. Faucher
Institut Carnot de Bourgogne, UMR 5209 CNRS-Université de Bourgogne, 9 Av. A. Savary, BP 47 870, 21078 Dijon Cedex, France

P. Tzallas (✉) · E.P. Benis · J. Kruse · A. Peralta Conde · C. Kalpouzos · D. Charalambidis
Foundation for Research and Technology-Hellas, Institute of Electronic Structure and Laser, P.O. Box 1527, 71110 Heraklion, Crete, Greece
e-mail: ptzallas@iesl.forth.gr

D. Charalambidis
Department of Physics, University of Crete, P.O. Box 2208, 71003 Heraklion, Crete, Greece

the inclusion of the spatial displacement in our model is expected not only to put under stringent tests the applicability of the 2nd order AC approach but also provide us with substantial information about the restrictions of the method. Indeed, the inclusion of the spatial displacement becomes compulsory when the spatial length of the pulse to be characterized becomes comparable to the confocal parameter of the foci. While the effect of this displacement seems in principle negligible for few-fs or sub-fs pulses, it is not obvious how it may affect the 2nd order AC trace in tight focusing geometries (indispensable to 2nd order AC of VUV-EUV pulses) of pulses longer than several tens of fs. In addition, the 2nd order AC approach can be used in studying, simultaneously with the pulse characterization, the dynamics of many ultra-fast processes in photochemistry, since most of the organic compounds absorb in the VUV-EUV spectral region [12]. In this approach, the AC trace is a convolution of both the pulse duration and the characteristic decay times of the photochemical processes under investigation and may well exceed a hundred of fs in duration, thus suffering from the effects of spatial displacement. Since no investigations have been reported on this displacement issue up to now, at least to our knowledge, the introduced model is expected to provide us with the appropriate conditions for safely applying the 2nd order AC method to the characterization of UV-EUV pulses. Based on the above investigations, a high accuracy measurement of the duration of the 5th harmonic of a 50 fs long laser pulse including the carrier wavelength oscillation is presented. Earlier measurements of the 5th harmonic through alternative approaches can be found in [13] and [14].

2 Theoretical treatment

The theoretical description of the non-linear autocorrelator is based on the description of the three-dimensional light distribution near focus presented in detail in [15], and adapted here for the geometry shown in Fig. 1. The harmonic field E, reflected by the split spherical mirror, is obtained as the superposition of the two fields E_i, with $i = 1$ and 2, corresponding to the reflected parts from each half of the split mirror, respectively. Assuming Gaussian temporal profiles and propagation along the z-direction, the fields are written

$$E_i(x, y, z, t) = E_{i0}(x, y, z) \exp\left(-2 \ln 2 \left(\frac{t}{\tau_p}\right)^2\right) \times \exp\big(i\omega(t)\big),$$

where τ_p is the pulse duration, ω is the field carrier angular frequency and $E_{i0}(x, y, z)$ is the spatial distribution of the complex field. The spatial distribution of the field amplitudes at a certain space point P_2 in the neighborhood of the focal point $O(x = y = z = 0)$, is obtained by the Debye integral [15], after applying the Huygens–Fresnel principle in a small angles geometry, as

$$E_{i0}(P_2) = \frac{-i}{\lambda} \iint_{\Omega_i} A(P_1) \exp\big(i\phi_i(P_1)\big) \exp(-ik\hat{s}\mathbf{R})\, d\Omega,$$

k and λ are the wave vector and the wavelength of the radiation, respectively, while Ω corresponds to the solid angle which one half of the split mirror subtends at the focal point O. As shown in Fig. 1, the position vector $\mathbf{R}$ specifies the position P_2 relative to the origin O, while $\hat{s}$ is the position unit vector that specifies the position P_1 on the surface of the split mirror relative to O. $A(P_1)$ is the incident field amplitude at P_1. It is considered Gaussian $A(r) = A_0 \exp(-\frac{r^2}{w^2(r)})$, with $r^2 = x^2 + y^2$, w the beam radius and A_0 a constant factor. ϕ_i represents the phase of the incoming beam at the surface of the split mirror.

Considering all the above, the 2nd order volume AC trace of the harmonic field E is obtained as a function of the delay $\tau = 2\delta/c$, where δ is the displacement between the two

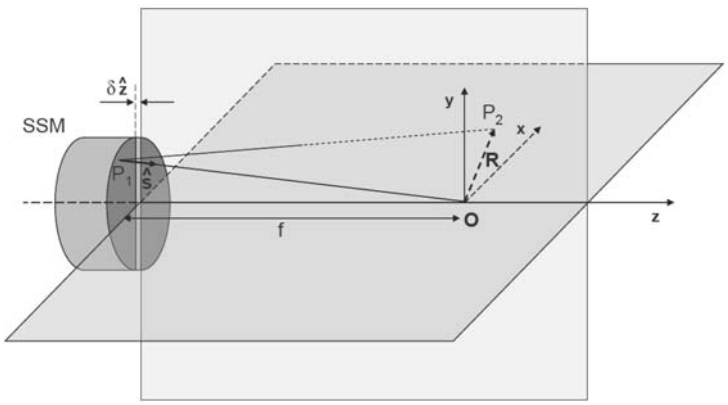

Fig. 1 Schematics of the model optical geometry. SSM: Split Spherical Mirror

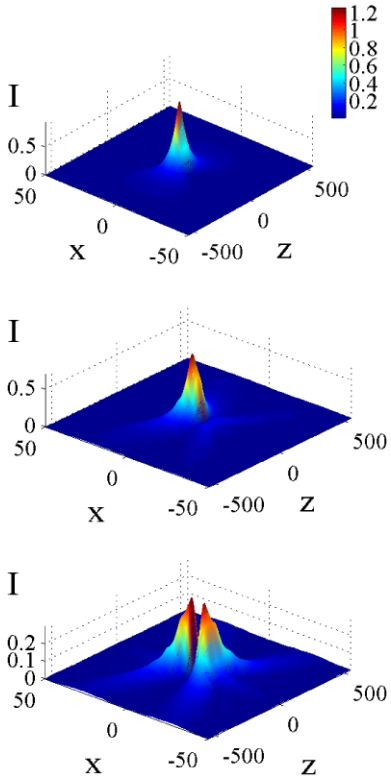

Fig. 2 Intensity distributions at the focus of a split spherical mirror for the displacement delays of: (*top*) zero, (*middle*) $\lambda/4$ and (*bottom*) $\lambda/2$. X and Z-axis are both in units of the wavelength λ, while the intensity I is in arbitrary units. The Z-axis is the axis of propagation

halves of the split mirror and c the speed of light, as

$$S(\tau) = \int dt \iiint dx\, dy\, dz \left| E(x, y, z, t) + E(x, y, z, t - \tau) \right|^4.$$

S has been calculated over a rectangular parallelepiped volume of width $20w_0$ and length $6.5b$, with w_0 and b being the beam waist and the confocal parameter of the Gaussian harmonic field, respectively.

Finally, the intensity distributions at the focus of a split spherical mirror for the displacement delays of zero, $\lambda/4$ and $\lambda/2$ are illustrated in Fig. 2.

3 Experiment

The experimental set-up is shown in Fig. 3. A 10 Hz Ti:Sapphire laser system delivering 50 fs pulses with energy up to 150 mJ and carrier wavelength at 800 nm was used. An annular laser beam with 2 cm outer diameter and energy of 15 mJ/pulse was focused by a 3.5 m focal length lens into a pulsed Xe gas jet, generating harmonics. After the jet an iris stopped the IR beam, while a Si plate was placed at the

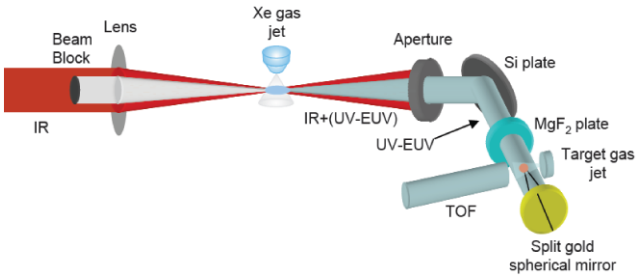

Fig. 3 Schematics of the non-linear volume AC apparatus

fundamental's Brewster angle of 72°, blocking the residual IR radiation and reflecting the harmonics towards the interaction chamber [16]. The harmonic beam was subsequently focused into a Kr gas jet, by a wave-front splitting arrangement consisting of a bisected gold spherical mirror of 5 cm focal length, the one half of which served as the translation unit. The translation is succeeded via a dual system of piezoelectric crystals (coarse and fine combination) allowing for a total stroke of 500 fs and a minimum resolution of 10 as. The 5th harmonic two-photon non-resonant ionization of Kr was used as the non-linear detector.

Kr is ionized by 5th harmonic two-photon absorption (IP = 13.995 eV) [17]. In order to avoid unwanted contributions from single-photon ionization by photons of the 9th and higher harmonics, a 5 mm thick MgF_2 plate was introduced in the harmonic beam filtering out all wavelength contributions shorter than 113 nm. The MgF_2 plate acted also as a temporal separator for the harmonics since the group velocity and the group velocity dispersion are different for each harmonic. Since the various harmonics are temporally separated and all possible multi-photon absorption channels are non-resonant, color-mixing channels do not contribute to the excitation processes and the excited population follows instantaneously the variations of the harmonic fields [18–20]. In addition, the driving laser pulse was stretched properly in order to compensate for the chirp introduced to the 5th harmonic by the MgF_2 plate, thus leading to a Fourier-transform limited (FTL) 5th harmonic pulse. As a result, the durations of the surviving harmonics other than the 5th become much longer than that of an FTL value, much too long to account for a 2nd order process. In a step further, it has been estimated that under the present experimental conditions the intensities of the 3rd and 5th harmonic are approximately the same at the interaction region. Since at such intensities the 3rd harmonic three-photon ionization rate is much smaller than that of the 5th harmonic two-photon ionization, it can be safely deduced that the contribution of the 3rd harmonic to the ionization signal is negligible.

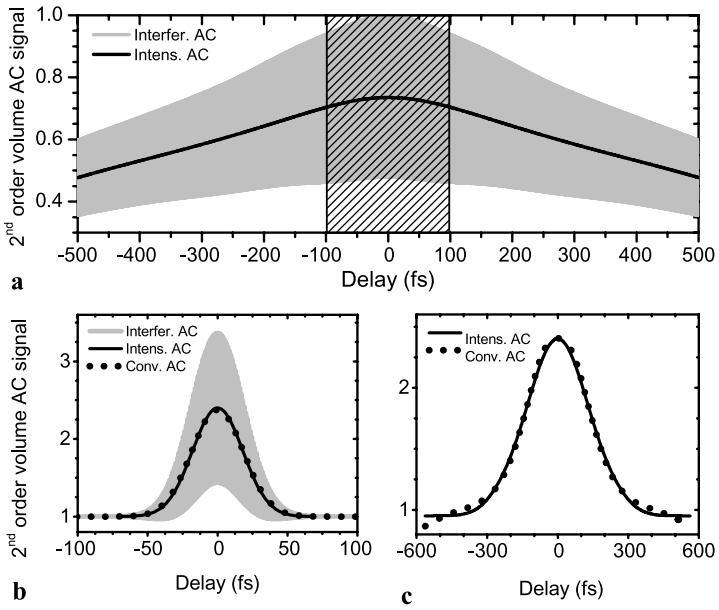

Fig. 4 Model calculations of the 2nd order volume interferometric (*grey shaded areas*) and intensity (*black solid lines*) AC traces for a (**a**) CW laser, (**b**) 30 fs, and (**c**) 200 fs pulses. *Black dots*: conventional 2nd order intensity volume AC traces. The 200 fs *shadowed area* in Fig. 3a depicts the area of negligible (<5%) deviation of the AC signal due to spatial displacement for the tight focusing conditions considered here (see text for details)

4 Results and discussion

Figure 4a illustrates an instructive example that sheds light onto the effects of displacement present in the autocorrelation method. Assuming a realistic tight focusing condition of 5 cm focal length for a bisected spherical mirror and a CW laser pulse, we performed calculations based on the presented model for the 2nd order volume AC. The grey shaded area corresponds to the interferometric trace, while the black solid line corresponds to the intensity trace. A clear reduction of the signal from its maximum value, which is supposed to be constant for a CW laser, is evident, and is due to the spatial separation of the two foci of the two halves of the split mirror in the focal area. Specifically, a reduction of 5% is evident for a spatial displacement corresponding to 100 fs from both sides of the zero delay (shadowed area in Fig. 4a). Even though the reduction for this delay region is negligible, the displacement effects become increasingly important for longer delays in such tight focusing conditions and should be considered accordingly.

Figure. 4b and c show two realistic examples involving the model calculations of a 30 and 200 fs duration Gaussian laser pulses, respectively, at the same geometrical and focusing conditions as in Fig. 4a. The grey shaded area corresponds to the interferometric trace, while the black solid lines correspond to the intensity trace. The black dots correspond to the conventional 2nd order intensity volume AC trace, i.e., a 2nd order intensity volume AC trace that does not take into account the displacement. As is seen in Fig. 4b, for the case of 30 fs pulse the conventional intensity volume AC trace is exactly the same with the model calculations of the intensity volume AC trace. In addition, a Gaussian function (not shown in the graph) perfectly fits to these traces. This is because the variation of the signal due to the displacement of the foci is negligible in the scanning area of -100 to $+100$ fs (shadowed area in Fig. 4a), as it is inferred form Fig. 4a. However, in the case of a 200 fs pulse, deviations start to appear at the tails of the trace, as shown in Fig. 4c. Therefore, in the case of pulses longer than 200 fs, it is necessary to de-convolve the AC trace from the function which describes the dependence of the ion signal due to the displacement of the foci, in order to extract the duration of the pulse. This new finding adds complementarity to the studies of previous three-dimensional [2], two-dimensional [21] and quasi-three-dimensional [22] works, in which the displacement of the two foci was justifiably ignored as is now confirmed redundant for the given experimental conditions.

Based on the results shown in Fig. 4b, the trace contrasts, defined as the peak to background ratios in the cases of intensity and interferometric volume 2nd order AC traces, are obtained as 2.4 and 3.4, respectively, which are values slightly higher than those reported in [2]. However, it has been numerically verified that in the limit of infinite integration volume the aforementioned ratios are reduced to 2.1 and 2.8, respectively, in agreement with the values given in [2]. In addition, the modulation depth, which is defined as $M \equiv 2(S_{\max} - S_{\min})/(S_{\max} + S_{\min})$, is measured to be $M = 0.8$. Finally, the deconvolution factor, which is the ratio of AC width (FWHM) to the original pulse width (FWHM), reads 1.51 for the interferometric AC, while it is reduced to 1.41 for the intensity AC case, in accordance to previous studies [21], as the inclusion of the displacement should not affect the above results for such short pulses.

The same values are obtained from the 200 fs pulse duration case, which in principle shows that the displacement af-

fects the measured duration negligibly. However, the above measurement is valid only because we were precisely aware of the background AC signal value. In realistic conditions, the background AC baseline would not maintain a constant value, as clearly shown in Fig. 4c, but rather one reduced with a delay value. Therefore, an effortless Gaussian fit may very well lead to an inaccurate pulse duration extraction. In such cases only the inclusion of displacement in a model calculation would safely account for the pulse duration extraction from the AC trace.

It is of significant importance to emphasize at this point that all the above analysis is valid for pulses with durations close to their Fourier-transform limited (FTL) value. For non-FTL pulses, the presence of chirp is responsible for the appearance of wings at the tails of the AC trace, a fact that complicates the situation and is not included in our study. This point indicates that in order to observe non-negligible effects due to the inherent displacement in the 2nd order volume AC approach, FTL pulses of durations longer than 200 fs for tight focusing geometries are needed. Considering the fact that nowadays the majority of the fs laser installations worldwide involve laser FTL pulses of less than 50 fs durations, it becomes unrealistic to meet the conditions for observing the displacement effects in 2nd order AC traces, except maybe in the XFEL installations that still involve pulses longer than 100 fs. However, inverting the argument, the above reasoning implies that the 2nd order volume AC approach can be safely applied by the laboratories worldwide to directly and accurately obtain the generated harmonic pulses duration as long as the intensity required is available.

Following this path, which is establishing the negligibility of the displacement effects on the 2nd order AC trace for pulses of a few tens of fs duration, the duration of the 5th harmonic of a Ti:Sapphire laser has been accurately determined utilizing the 2nd order volume AC measurements shown in Fig. 5. The two-photon ionization signal of Kr is plotted as a function of the delay τ between the two 5th harmonic pulses of a Ti:Sapphire laser pulse with 50 fs duration over an interval of 250 fs with a step of 3.3 fs (open circles). For each delay step 125 laser shots were accumulated. A Gaussian fit (dash line) to the data results in a duration of 27.3 ± 0.7 fs, which is a value close to the FTL value of 22.4 fs. A model calculation for the 2nd order volume AC trace involving a pulse of 27.3 fs duration and accounting for the measured trace contrast is shown in Fig. 5 (grey solid line) depicts no essential deviation from the Gaussian fit, as was expected. The measured peak to background ratio is found to be 1.8, which is close to the calculated value of 2.1, the deviation attributed primarily to the imperfect overlap of the two beams at the focal area.

In a step further, the oscillation of the ion yield at the 5th harmonic field frequency was recorded and is shown in the

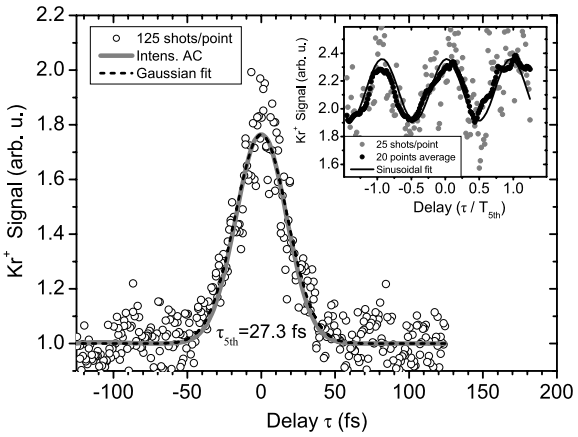

Fig. 5 *Open circles*: measured 2nd order volume AC trace of the 5th harmonic. *Grey solid line*: simulated 2nd order volume AC trace. *Dash line*: Gaussian fit. The measured 2nd order interferometric volume AC trace is shown in the *inset*. *Grey dots*: experimental data. *Black dots*: running average over 20 data points. *Black solid line*: sinusoidal fit to the averaged data

inset of Fig. 5. In this trace the delay step is 10 as, while for each point of the trace 25 shots were accumulated (grey dots). A running average of 20 data points is shown in blue dots. The averaged data were fitted to a sinusoidal function (black line) resulting in a period of 540 ± 30 as. This result establishes access to sub-500 as resolution for our detection apparatus in a spectral region of high interest to ultra-fast photochemical processes. The modulation depth of the oscillations in the interferometric AC trace reads $M = 0.22$, which is 3.6 times smaller than the calculated value of 0.8. This divergence is attributed to laser pulse energy instabilities and/or the spatial chirp of the 5th harmonic across the beam cross section at the focus. It is worth noticing here that the coarse and fine scan traces correspond to a different set of data and thus to possibly slightly different beam stability conditions. For this reason the noise level of the two traces is not directly comparable. However we should clarify that the fluctuations in the coarse scan are not purely due to noise, but are so to a large extent, because the measured points correspond to quasi randomly chosen points of an interferometric trace. Thus, the modulation inherent in an interferometric trace appears as a strongly fluctuating trace in a coarse scan.

5 Conclusions

Model calculations for the 2nd order AC approach that include three-dimensional integration over a large ionization volume, temporal delay and spatial displacement of the two beams of the autocorrelator at the focus were presented. The effects of the displacement inherent to the 2nd order AC approach were exposed by certain examples elucidating the restrictions of the 2nd order AC approach in tight focusing

conditions. In general, the 2nd order AC approach can be safely applied for pulses with a duration of up to few tens of fs, however, special care should be taken in the pulse duration extraction in cases where the pulse duration exceeds the order of 100 fs. The same applies to 2nd order AC traces that involve convolution of both the pulse duration and the characteristic decay times of photochemical processes. The negligibility of the displacement effect was demonstrated experimentally. A 2nd order volume AC measurement of the duration of the 5th harmonic of a 50 fs long laser pulse was performed, depicting identical results between a Gaussian fit and the model calculations. The pulse duration of the 5th harmonic was measured to be 27.3 ± 0.7 fs. The fast oscillations of the AC trace in the sub-fs temporal regime were also recorded, resulting in a 5th harmonic period of 540 ± 30 as.

Acknowledgements This work is supported in part by the European Community's Human Potential Program under contract MTKD-CT-2004-517145 (X-HOMES); the Ultraviolet Laser Facility (ULF) operating at FORTH-IESL (contract No. HPRI-CT-2001-00139).

References

1. P. Tzallas, D. Charambidis, N.A. Papadogiannis, K. Witte, G.D. Tsakiris, Nature (Lond.) **426**, 267 (2003)
2. P. Tzallas, D. Charalambidis, N.A. Papadogiannis, K. Witte, G.D. Tsakiris, J. Mod. Opt. **52**, 321 (2005)
3. Y. Nabekawa, T. Shimizu, T. Okino, K. Furusawa, H. Hasegawa, K. Yamanouchi, K. Midorikawa, Phys. Rev. Lett. **96**, 083901 (2006)
4. P.B. Corkum, F. Krausz, Nature (Lond.) Phys. **3**, 381 (2007)
5. M.F. Kling, M. Vrakking, Annu. Rev. Phys. Chem. **59**, 463 (2008)
6. P. Farnamara, O. Steinkellner, M.T. Wick, M. Wittmann, G. Korn, V. Stert, W. Radloff, J. Chem. Phys. **111**, 14 (1999)
7. K. Kosma, S.A. Trushin, W. Fuss, W.E. Schmid, J. Phys. Chem. A **112**, 7514 (2008)
8. S. Witte, R.Th. Zinkstok, W. Hogervorst, W. Ubachs, K.S.E. Eikema, Opt. Express **14**, 8168 (2006)
9. F. Tavella, Y. Nomura, L. Veisz, V. Pervak, A. Marcinkevicius, F. Krausz, Opt. Lett. **32**, 2227 (2007)
10. P. Tzallas, E. Skantzakis, C. Kalpouzos, E.P. Benis, G.D. Tsakiris, D. Charalambidis, Nat. Phys. **3**, 846 (2007)
11. D. Oran, Y. Silberberg, N. Dudovich, D.M. Villeneuve, Phys. Rev. A **72**, 063816 (2006)
12. A. Peralta Conde, J. Kruse, O. Faucher, P. Tzallas, E.P. Benis, D. Charalambidis (2009, submitted)
13. T. Sekikawa, T. Ohno, T. Yamazaki, Y. Nabekawa, S. Watanabe, Phys. Rev. Lett. **83**, 2564 (1999)
14. T. Sekikawa, T. Katsura, S. Miura, S. Watanabe, Phys. Rev. Lett. **88**, 193902 (2002)
15. M. Born, E. Wolf, *Principles of Optics* (Pergamon, New York, 1968)
16. E.J. Takahashi, H. Hasegawa, Y. Nabekawa, K. Midorikawa, Opt. Lett. **29**, 507 (2004)
17. D. Descamps, L. Roos, C. Delfin, A. L'Huillier, C.G. Wahlstrom, Phys. Rev. A **64**, 031404(R) (2001)
18. L.A.A. Nikolopoulos, E.P. Benis, P. Tzallas, D. Charalambidis, K. Witte, G.D. Tsakiris, Phys. Rev. Lett. **94**, 113905 (2005)
19. D. Charalambidis, P. Tzallas, E.P. Benis, E. Skantzakis, G. Maravelias, L.A.A. Nikolopoulos, A. Peralta Conde, G.D. Tsakiris, New J. Phys. **10**, 025018 (2008)
20. A. Peralta Conde, P. Tzallas, D. Charalambidis, Eur. Phys. J. D **51**, 289 (2009)
21. H. Mashiko, A. Suda, K. Midorikawa, Appl. Phys. B **76**, 525 (2003)
22. H. Mashiko, A. Suda, K. Midorikawa, Appl. Phys. B **87**, 221 (2007)